

# Observation of Coulomb Gap and Enhanced Superconducting Gap in Nano-Sized Pb Islands Grown on SrTiO<sub>3</sub> \*

Yonghao Yuan(袁永浩)<sup>1,2</sup>, Xintong Wang(王心童)<sup>1,2</sup>, Canli Song(宋灿立)<sup>1,2</sup>, Lili Wang(王立莉)<sup>1,2</sup>,  
Ke He(何珂)<sup>1,2</sup>, Xucun Ma(马旭村)<sup>1,2</sup>, Hong Yao(姚宏)<sup>1,2,3</sup>, Wei Li(李渭)<sup>1,2\*\*</sup>, Qi-Kun Xue(薛其坤)<sup>1,2,4\*\*</sup>

<sup>1</sup>State Key Laboratory of Low-Dimensional Quantum Physics, Department of Physics,  
Tsinghua University, Beijing 100084

<sup>2</sup>Frontier Science Center for Quantum Information, Beijing 100084

<sup>3</sup>Institute for Advanced Study, Tsinghua University, Beijing 100084

<sup>4</sup>Beijing Academy of Quantum Information Sciences, Beijing 100193

(Received 10 December 2019)

We report high-resolution scanning tunneling microscopy (STM) study of nano-sized Pb islands grown on SrTiO<sub>3</sub>, where three distinct types of gaps with different energy scales are revealed. At low temperature, we find that the superconducting gap ( $\Delta_s$ ) in nano-sized Pb islands is significantly enhanced from the one in bulk Pb, while there is no essential change in superconducting transition temperature  $T_c$ , giving rise to a larger BCS ratio  $2\Delta_s/k_B T_c \sim 8.31$  and implying stronger electron-phonon coupling. The stronger coupling can originate from the interface electron-phonon interactions between Pb islands and SrTiO<sub>3</sub>. As the superconducting gap is totally suppressed under applied magnetic field, the Coulomb gap with apparent V-shape emerges. Moreover, the size of Coulomb gap ( $\Delta_C$ ) depends on the lateral size of Pb islands ( $R$ ) with  $\Delta_C \sim 1/R^{0.35}$ , indicating that quantum size effect can significantly influence electronic correlations. Our experimental results shall shed important light on the interplay among superconductivity, quantum size effect and correlations in nano-sized strong-coupling superconductors.

PACS: 74.78.-w, 74.78.Na, 74.55.+v, 73.22.-f, 73.23.Hk

DOI: 10.1088/0256-307X/37/1/017402

Electronic properties in quantum materials may be qualitatively modified by reducing their size and/or dimensions, which have attracted extensive interests in condensed matter physics research. One intriguing discovery in size confined systems is the enhancement of superconductivity in nano-sized weak coupling superconducting films, such as Al, In and Sn.<sup>[1,2]</sup> The mechanism of enhanced superconductivity has been explained as surface phonon softening,<sup>[3]</sup> which leads to the enhanced electron-phonon coupling based on Eliashberg theory.<sup>[4,5]</sup> In contrast,  $T_c$  of strong coupling superconductors, like Pb, is hardly boosted by reducing their size. Actually, in two-dimensional Pb films grown on Si(111),  $T_c$  shows oscillating decrease tendency with the decreasing film thickness.<sup>[6,7]</sup> To obtain enhanced surface phonon coupling, Pb nanoparticles with higher surface-area ratio are prepared, in which the  $T_c$  presents a constant value (still lower than that of bulk Pb) with the size reduction until approaching the Anderson limit.<sup>[8,9]</sup>

When their sizes are smaller than the Anderson limit ( $\sim 10$  nm), both the weak and strong coupling superconductors lose their superconductivity.<sup>[10]</sup> In this zero-dimensional limit, extreme electronic correlation dominates and induces Coulomb blockade phenomenon. Indeed, studies on nano-sized silver particles<sup>[11]</sup> and graphene nano-ribbons<sup>[12]</sup> have shown

that Coulomb interaction is significantly enhanced during size reduction, which may even induce metal-insulator transition. Besides the electron-electron interaction, electron-phonon interaction is modified by size effect as well, manifesting as pseudogap feature observed in Pb islands.<sup>[13]</sup> Therefore, electronic properties of low-dimensional superconductors are more complicated than expected, and we need to revisit the influences of both Coulomb and electron-phonon interactions in those systems.

It has been experimentally established that superconductivity can be significantly enhanced in a monolayer FeSe film grown on SrTiO<sub>3</sub>,<sup>[14]</sup> demonstrating that metal-oxide interface could be another key factor to boost  $T_c$ .<sup>[14–16]</sup> Hence, by constructing a new system that can combine all those factors together, it would provide an ideal platform to study their interplay with two-dimensional superconductivity.

In this Letter, we report on molecular beam epitaxy (MBE) growth and systematic STM studies of laterally confined Pb islands on SrTiO<sub>3</sub>(001) (Pb/STO). Three distinct types of energy gaps have been observed, which are the superconducting gap, Coulomb gap, and pseudogap. They manifest themselves in different energy scales. At low temperature, the superconducting gap in Pb/STO is enlarged, with the gap size ( $\Delta_s$ ) of  $\sim 2.50$  meV, larger than 1.36 meV

\*Supported by the National Natural Science Foundation under Grant Nos. 11674191 and 11825404, the National Key Program for S&T Research and Development under Grant No. 2016YFA0301002, and the Beijing Advanced Innovation Center for Future Chip (ICFC). W.L. was also supported by Beijing Young Talents Plan.

\*\*Corresponding authors. Email: weili83@tsinghua.edu.cn; qkxue@mail.tsinghua.edu.cn

© 2020 Chinese Physical Society and IOP Publishing Ltd

for bulk Pb. However, the  $T_c$  in Pb/STO is not enhanced from the bulk value, giving rise to a larger BCS ratio  $2\Delta_s/k_B T_c \sim 8.31$  in the nano-sized Pb/STO. When the superconductivity is suppressed under applied magnetic field, Coulomb gap ( $\Delta_C \sim 1$  meV) induced by electronic interaction is clearly revealed. The value of Coulomb gap increases with reduction of the lateral size of Pb islands. As the lateral size approaches the Anderson limit, Coulomb blockade feature starts to appear. Finally, a pseudogap  $\Delta_p$  with the magnitude of  $\sim 10$  meV, at rather larger energy scale, is visible (even at 30 K), which may originate from the weakening of electron-phonon interaction.<sup>[13]</sup>

Figure 1(a) shows a typical STM topographic image of Pb islands grown on the SrTiO<sub>3</sub> (STO) substrate. The atomic resolution result (see Section 1 in the Supplementary Material) shows hexagonal lattice with lattice constant of 3.49 Å on Pb islands, in good agreement with that of the (111) surface of FCC-phase Pb. The lattice constant of STO is 3.9 Å. Due to the large lattice mismatch as well as the decomposed surface oxygen of STO during the Pb growth, the growth follows the Stranski–Krastanov mode (i.e., islands start to form after the growth of a wetting layer of Pb) and the wetting layer is much rougher than that of Pb grown on Si (111). Three types of Pb islands classified as A, B and C are obtained. The type-A islands are thicker than 15 nm, and exhibit the superconducting gap similar to that of bulk Pb (see Fig. 1(b)). The U-shaped superconducting gap is fitted well by the Dynes model,<sup>[17]</sup> and the fitted gap value is 1.36 meV with scattering rate  $\Gamma_A \sim 0.08$  meV, consistent with that of its bulk material.

The heights of type-B Pb islands are 3–8 nm and their areas range from 1000 nm<sup>2</sup> to 100000 nm<sup>2</sup>. The  $dI/dV$  spectrum shows a larger superconducting gap but with lower coherence peaks (Fig. 1(c)). The fitting result suggests that the magnitude of the enlarged superconducting gap  $\Delta_s$  is 2.58 meV and the corresponding scattering rate  $\Gamma_B$  is 0.24 meV. Systematic study on the enlarged superconducting gap is shown in Section 2 in the Supplementary Material. The well-defined superconducting gap enlargement of Pb has not been reported yet, and we attribute the origin of the gap enhancement here to the special substrate (STO) used. The STO-Pb interface may provide additional electron-phonon coupling channel to enhance the superconducting pairing strength. The fitting curve deviates from the data at the bottom of the gap near the Fermi level ( $E_F$ ), implying the existence of non-BCS behaviors in the type-B islands. Type-C islands are of the smallest size, usually smaller than 500 nm<sup>2</sup>. The  $dI/dV$  spectrum (Fig. 1(d)) shows several discrete peaks, which are signatures for Coulomb blockade.<sup>[18]</sup> The Coulomb blockade can be observed here owing to the imperfect interface between STO and Pb. Meanwhile, superconductivity here is absent due to approaching of the Anderson limit.<sup>[10]</sup> Since

type-B islands present the most intriguing electronic properties, we mainly focus on this type of Pb islands in our following discussion.

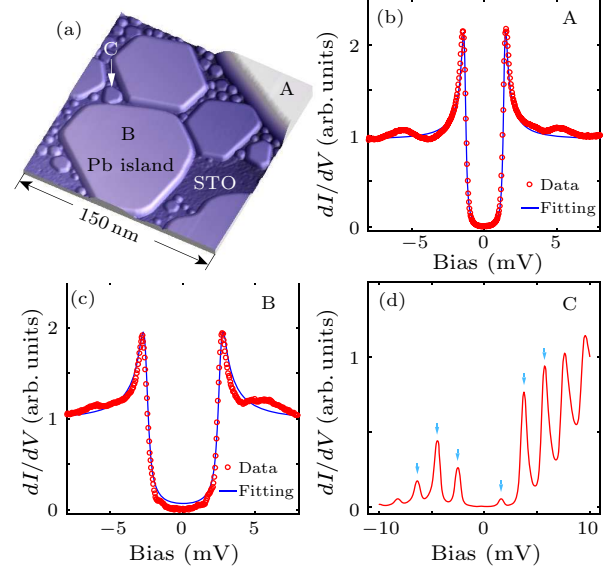


**Fig. 1.** (a) STM topographic image of Pb islands grown on the STO(001) substrate (150 nm × 150 nm). Set point: bias voltage  $V_s = 2.0$  V, tunneling current  $I_t = 20$  pA. [(b), (c)] The  $dI/dV$  spectra taken on type-A and type-B Pb islands grown on STO substrates, respectively (400 mK,  $V_s = 10$  mV,  $I_t = 400$  pA). The data are presented with red circles, and the fitting results by the Dynes model are in blue curves. Type-A islands behave like bulk Pb and show a 1.36-meV superconducting gap. Type-B islands show an enlarged 2.58-meV gap. (d) The  $dI/dV$  spectra taken on a type-C Pb island (400 mK,  $V_s = 10$  mV,  $I_t = 400$  pA). The discrete peaks, denoted by cyan arrows, are signatures of Coulomb blockade.

Superconducting gaps of type-B Pb islands are strongly suppressed by externally applied magnetic field. Figure 2(a) exhibits the  $dI/dV$  spectra taken on an island with applying various perpendicular magnetic fields. The effective radius ( $R$ ) of the island is  $\sim 32.8$  nm, where  $R$  is estimated by the formula  $R = (\text{area}/\pi)^{1/2}$ . The superconducting gap keeps shrinking with increasing applied magnetic fields and persists even up to 0.75 T, indicating an enhancement of upper critical field of the Pb islands compared with its bulk value  $\sim 0.08$  T. Remarkably, the gap feature is no longer sensitive to magnetic field from 1.5 T and such a residual gap is unchanged up to 15 T. The magnitude of this field insensitive gap  $\Delta_C$  is  $\sim 0.65$  meV (see Fig. 2(a) and Fig. S3).

The residual gaps are V-shaped (see Figs. 2(a) and 2(b)) and the density of states (DOS) exhibits a linear dependence on energy near  $E_F$  (see Figs. S3 and S4). Theoretical work has proposed that in two-dimensional correlated systems, Coulomb gap may develop and the DOS of corresponding electrons near  $E_F$  linearly depend on energy:  $G \sim |E|$ .<sup>[19]</sup> Therefore, the residual gap here may be Coulomb gap induced by electronic correlation. Previous studies on

Coulomb gap mainly focused on amorphous metals<sup>[20]</sup> and doped semimetals,<sup>[21]</sup> in which variable range hopping of localized electrons with poor screening dominates the conductivity. By reducing the size of a Pb island to cross from two-dimensional to zero-dimensional limit, Coulomb gap becomes pronounced for the following reasons: (i) Coulomb interaction affects in longer range according to the Lindhard screening theory.<sup>[22]</sup> (ii) The itinerant *s*-electrons have spill-out effect, which further weakens the screening effect on smaller islands.<sup>[23]</sup> When the values of  $\Delta_C$  and  $\Delta_s$  are comparable in a low-dimensional system, another interesting phenomenon is the possible change of effective charge of a single electron, which still requires further investigations.<sup>[24]</sup>

To investigate the relationship between the Coulomb gap and the size of Pb islands, a series of  $dI/dV$  spectra (Fig. 2(b)) are taken on various Pb islands. High magnetic fields are applied to suppress the superconducting gap and highlight the Coulomb gap. As is expected,  $\Delta_C$  becomes larger and deeper as  $R$  decreases, showing that Coulomb interaction is indeed affected by size effect and is more pronounced in smaller islands. Based on the fitting of our results, the Coulomb gap size ( $\Delta_C$ ) has a power-law dependence on  $R$ :  $\Delta_C \sim 1/R^{0.35}$ .  $\Delta_C$  and  $R$  are plotted out in logarithmic scales in Fig. 2(c), where the exponent 0.353 is obtained from the slope of the fitting curve. Similarly, as shown in Fig. 2(d), the logarithmic zero energy density of states ( $G_0$ ) obeys  $\ln G_0 \sim -1/R^{1.91}$ , where the exponent 1.91 is very close to 2, indicating  $G_0$  decays exponentially with  $1/\text{area}$ . It is noteworthy that the spectrum on a small island with  $R = 23.1$  nm shows a harder gap and several peak feature (denoted by cyan arrows in Fig. 2(b)) outside the gap, indicating that the system approaches Coulomb blockade regime (like type-C islands) as the lateral size of island keeps decreasing. Pb islands were grown on SrTiO<sub>3</sub> substrates with different Nb doping levels (0.7%, 0.25% and 0.15%), while the data taken on those substrates obey the same fitting curve (see the data points with different color in Fig. 2(b)–2(d)), demonstrating that the Coulomb gap is not sensitive to the details of substrates as well as their interfaces. We note that a previous study has also found an area-dependent gap feature on Pb islands and explained it as dynamic Coulomb blockade phenomenon.<sup>[25]</sup> However, superconductivity of Pb is absent in that work, presenting a sharp distinction from our system.

We further studied magnetic field response on a larger type-B island ( $R \sim 83.7$  nm). Since the Bean-Livingston barrier<sup>[26]</sup> is overcome, a magnetic vortex is observed. Figure 3(a) shows the zero-bias  $dI/dV$  maps taken under different magnetic fields. The vortex emerges at 0.18 T and becomes blurred at 0.27 T. A linear fit on the extracted zero bias conductance values away from the vortex suggests an upper critical field ( $\mu_0 H_{c2}$ ) of 0.30 T (see Fig. S5).  $H_{c2}$  is determined

by the G-L coherence length  $\xi_{GL}$ :  $\mu_0 H_{c2} = \Phi_0/2\pi\xi_{GL}^2$ , where  $\Phi_0$  is magnetic flux quanta. Accordingly, the calculated coherence length  $\xi_{GL}$  is 33 nm, smaller than that of bulk Pb value (83 nm). A series of  $dI/dV$  spectra are taken across a vortex at 0.20 T and shown in Fig. 3(b). In the vortex core, a zero-bias peak originating from the Caroli-de Gennes-Matricorn bound states is clearly revealed, indicating that this two-dimensional superconducting system is in clean limit. In contrast, the superconducting Pb islands grown on Si (111) are always in dirty limit, and the bound states are absent in the vortex core.<sup>[27]</sup>

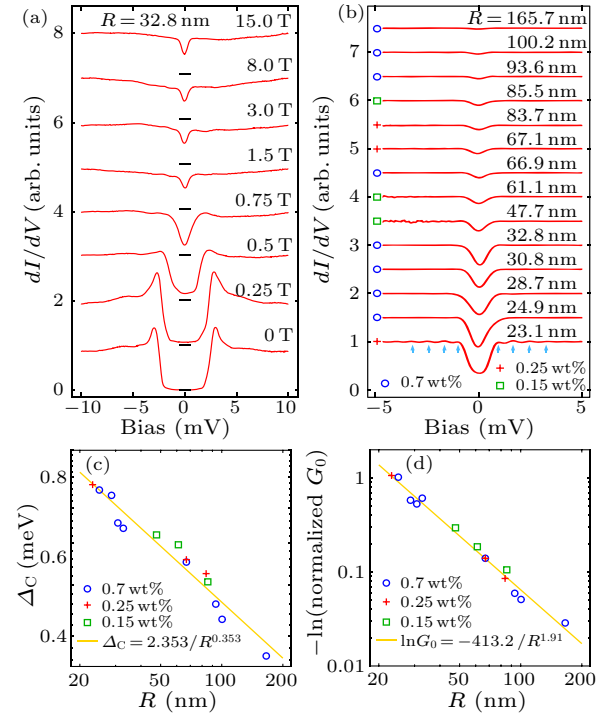


**Fig. 2.** (a) The  $dI/dV$  spectra taken on type-B Pb islands ( $R = 32.8$  nm) under various magnetic fields (400 mK,  $V_s = 10$  mV,  $I_t = 300$  pA). Upper critical field is enhanced, compared with that of bulk Pb. A residual gap still exists at high fields as superconductivity is totally suppressed. The magnetic insensitive residual gap is attributed to the Coulomb gap. (b) Coulomb gaps of Pb islands with different areas (for details, see Section 3 in the Supplementary Material). The blue circles, red crosses and green squares denote 0.7 wt%, 0.25 wt% and 0.15 wt% Nb-doped substrates, respectively. The cyan arrows denote the Coulomb blockade features. (c) Double logarithmic scale plot of Coulomb gap size and lateral size of Pb island. The fitting result suggests  $\Delta_C = 2.353/R^{0.35}$ . (d) Double logarithmic scale plot of negative logarithmic zero-energy density of states ( $-\ln G_0$ ) and lateral size of Pb island.  $G_0$  exponentially decays with  $1/\text{area}$ , which obeys  $G_0 = \exp(-413.2/R^{1.9})$ .

Our temperature-dependent measurements show that the superconducting gap is almost filled at 7.0 K (Fig. 3(c)). The fitting result suggests that the  $T_c$  is not higher than 7.3 K (see Fig. S6), which does not show significant enhancement compared with the  $T_c$  of bulk Pb. Intriguingly, the unchanged  $T_c$  associated with the enlarged superconducting gap  $\Delta_s$  leads

to a rather large BCS ratio ( $2\Delta_s/k_B T_c$ )  $\sim 8.31$ , close to the ratio in cuprates.<sup>[28]</sup> The enlarged BCS ratio indicates that Pb, an inherent strong coupling superconductor, becomes even more strong-coupled when grown on STO. The theoretical work has pointed out that the BCS ratio may be increased through the mechanism of surface phonon softening.<sup>[29]</sup> In our case, electron-phonon coupling on metal-oxide interface provides another possible channel to enhance the coupling strength.

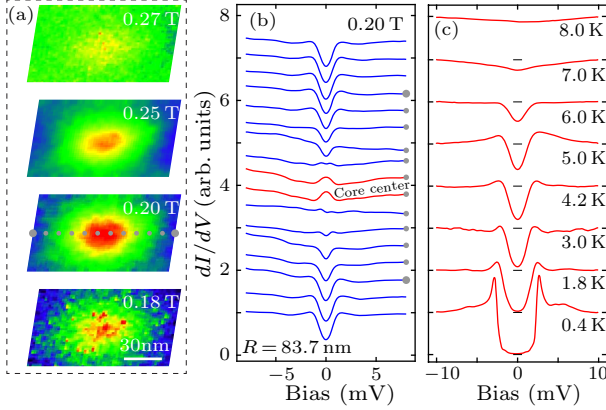


**Fig. 3.** (a) Zero-bias  $dI/dV$  maps taken on an  $R \sim 83.7$  nm island under different magnetic fields. The red color region, corresponding to higher conductance area, indicates the suppression of the superconducting gap and emergence of a vortex. (b) A series of  $dI/dV$  spectra taken across the vortex at 0.20 T (the corresponding positions are denoted by a grey dotted line in (a),  $V_s = 10$  mV,  $I_t = 200$  pA). A zero-bias peak is observed in the vortex core. (c) The  $dI/dV$  spectra taken on an  $R = 30.8$  nm Pb island at various temperatures ( $V_s = 10$  mV,  $I_t = 200$  pA). The superconducting gap is almost suppressed at 7.0 K, which does not show significant enhancement compared with that of bulk Pb.

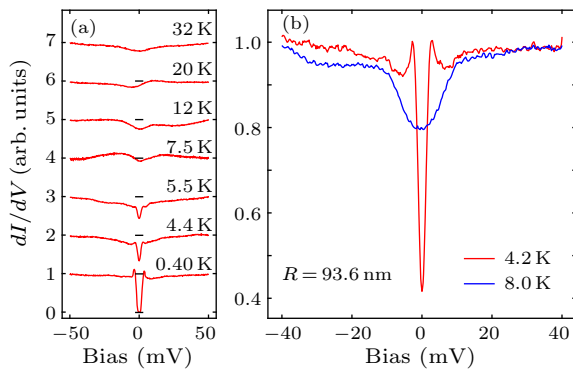


**Fig. 4.** (a) Larger-energy-range  $dI/dV$  spectra taken on an  $R \sim 100$  nm Pb island at various temperatures ( $V_s = 50$  mV,  $I_t = 200$  pA). When temperature is higher than  $T_c$ , a pseudogap persists near  $E_F$ . (b) Large range  $dI/dV$  spectra taken on an  $R = 93.6$  nm island ( $V_s = 50$  mV,  $I_t = 200$  pA). The red and blue curves show the spectra taken at 4.2 K and 8.0 K, respectively. The pseudogap coexists with the superconducting gap below  $T_c$ , as shown by the red curve.

Normal state of Pb islands is further investigated by larger energy range  $dI/dV$  spectra. As shown in Fig. 4(a), a larger gap  $\Delta_p$  with magnitude of  $\sim 10$  meV

is observed above  $T_c$  and even exists at 32 K. This pseudogap feature has already been studied in the Pb/Si system, explained as a modification to Fabry–Pérot mode due to the weakening of electron-phonon interaction below Debye energy.<sup>[13]</sup> A previous study on TiN has also found a pseudogap above  $T_c$ , which was explained as superconducting fluctuations.<sup>[30]</sup> According to our data, the pseudogap not only shows up above the  $T_c$ , but also coexists with the superconducting gap (see the dip features outside the superconducting gap in Fig. 4(b)). Therefore, the origin for the pseudogap observed in our study is probably not the superconducting fluctuation.

We have found that the superconducting pairing strength is significantly enhanced by STO substrate. The extra electron-phonon coupling channel on the Pb/STO interface is a possible explanation for the enhancement. However, the Coulomb interaction competes with the effect and probably hinders the boost of  $T_c$  in two ways. On the one hand, the Coulomb repulsion directly competes with the formation of Cooper pairs. On the other hand, the drop of DOS near  $E_F$  induced by the Coulomb gap restricts the potential of  $T_c$  enhancement. We demonstrate that the quantum size effect plays an important role to influence electronic correlation, which was usually ignored in two-dimensional superconducting systems in previous studies. Our finding sheds new light on understanding the interplay among superconductivity, quantum size effect, and complex electronic properties in low-dimensional quantum systems.

**Methods:** Our experiments were conducted in a commercial ultra-high vacuum STM (Unisoku), which is connected to an MBE chamber for sample preparation. In the MBE chamber, Nb-doped STO substrates were pre-treated at 1200°C to obtain TiO<sub>2</sub>-terminated surfaces. High-purity Pb (99.999%) was thermally evaporated from a standard Knudsen cell at 450°C. During the sample growth, the substrate was kept at room temperature. Our STM measurement was carried out at a base temperature of 400 mK. Vertical magnetic field up to 15 T can be applied. The  $dI/dV$  spectra were measured using the standard lock-in method with 973.0 Hz bias modulations.

## References

- [1] Cohen R W and Abeles B 1968 *Phys. Rev.* **168** 444
- [2] Bose S and Ayyub P 2014 *Rep. Prog. Phys.* **77** 116503
- [3] Watson J H P 1970 *Phys. Rev. B* **2** 1282
- [4] Eliashberg G 1960 *Sov. Phys.-JETP* **11** 696
- [5] McMillan W 1968 *Phys. Rev.* **167** 331
- [6] Guo Y et al 2004 *Science* **306** 1915
- [7] Eom D et al 2006 *Phys. Rev. Lett.* **96** 027005
- [8] Bose S et al 2009 *J. Phys.: Condens. Matter* **21** 205702
- [9] Vlaic S et al 2017 *Nat. Commun.* **8** 14549
- [10] Anderson P W 1959 *J. Phys. Chem. Solids* **11** 26
- [11] Voisin C et al 2000 *Phys. Rev. Lett.* **85** 2200
- [12] Han M Y et al 2007 *Phys. Rev. Lett.* **98** 206805
- [13] Wang K et al 2009 *Phys. Rev. Lett.* **102** 076801



- [14] Wang Q Y et al 2012 *Chin. Phys. Lett.* **29** 037402  
[15] Ginzburg V L 1964 *Phys. Lett.* **13** 101  
[16] Cohen M H and Douglass D H 1967 *Phys. Rev. Lett.* **19** 118  
[17] Dynes R C et al 1978 *Phys. Rev. Lett.* **41** 1509  
[18] Kastner M A 1992 *Rev. Mod. Phys.* **64** 849  
[19] Efros A and Shklovskii B 1975 *J. Phys. C* **8** L49  
[20] Butko V Y et al 2000 *Phys. Rev. Lett.* **84** 1543  
[21] Massey J G and Lee M 1995 *Phys. Rev. Lett.* **75** 4266  
[22] Lindhard J 1954 *K. Dan. Vidensk. Selsk. Mat. Fys. Medd.* **28** 8  
[23] Liebsch A 1993 *Phys. Rev. B* **48** 11317  
[24] Chen T et al 2012 *Phys. Rev. B* **86** 045135  
[25] Brun C et al 2012 *Phys. Rev. Lett.* **108** 126802  
[26] Bean C and Livingston J 1964 *Phys. Rev. Lett.* **12** 14  
[27] Nishio T et al 2008 *Phys. Rev. Lett.* **101** 167001  
[28] Fischer Ø et al 2007 *Rev. Mod. Phys.* **79** 353  
[29] Leavens C R and Fenton E W 1981 *Phys. Rev. B* **24** 5086  
[30] Sacepe B et al 2010 *Nat. Commun.* **1** 140  
[31] Bose S et al 2010 *Nat. Mater.* **9** 550